

UNIVERSITY GRANTS COMMISSION  
BAHADUR SHAH ZAFAR MARG  
NEW DELHI-110 002.

Final Report of the work done on the Minor Research Project.

1. Project report No.1<sup>st</sup>/Final : Final
2. UGC reference No.F. : MRP-6450/16(SERO/UGC)
3. Period of report: from : 01.09.2017 to 29.06.2019
4. Title of research project : *“Fabrication of Visible-light-driven Semiconductor Nanoheterostructures for the Enhanced Photocatalytic Treatment of Organic Contaminants in Aqueous Media”.*
5. (a)Name of the Principal investigator : Dr. S. Pitchaimuthu  
(b)Deptt. : Department of Chemistry,  
(c)College where work has progressed : Thiagarajar College, Madurai-9
6. Effective date of starting of the project : 01.09.2017
7. Grant approved and expenditure incurred during the period of the report
- a. Total amount approved Rs. : Rs. 1,60,000/-  
(Rs. 1,55,000 received)
- b. Total expenditure Rs. : Rs.1,58,476.00/-
- c. Report of the work done : Annexure-I  
(Please attach a separate sheet)
- i. Brief objective of the period :

1. The aims and objectives of the present proposed project are given below :

This proposal is enable the investigator for

- ✓ Developing semiconductor nanoheterostructures through suitable technique with enhanced photocatalytic efficiency compared with respective bare semiconductors.
- ✓ Characterize the prepared samples will be carried out by recording FESEM, PXRD, BETsurface area analysis, UV-Visible DRS, Photoluminescence emission spectra.

- ✓ To investigate the effects of various operating conditions like, concentration of pollutants, amount of catalyst, dose of catalyst, initial pH value, anionic species, addition of H<sub>2</sub>O<sub>2</sub>, etc. on the reaction rate.
- ✓ To study the photochemical removal of various groups of pollutants with different structure in aqueous solutions by photocatalysis.
- ✓ The decoloration kinetics of photodegradation of pollutants in water will be determine. To determine the rate constant for the removal of pollutants by photocatalysis using semiconductors based on Langmuir-Hinshelwood (LH) model under various experimental conditions. To characterize the reaction intermediates and to propose a possible reaction mechanism.

ii. Work done so far and results achieved and publications, if any, resulting from the work (Give details of the papers and names of the journals in which it has been

published or accepted for publication : Please refer Annexure-II

iii. Has the progress been according to

Original plan of work and towards

achieving the objective. If not, state reasons: Yes

iv. Please enclose a summary of the

Findings of the study. One bound copy

Of the final report of work done may also

be sent to the concerned Regional Office

of the UGC. : Summary attached

v. Any other information : Nil

SIGNATURE OF THE PRINCIPAL INVESTIGATOR

PRINCIPAL

(Seal)

**Papers presented in International conferences**

1. *National Seminar on Water Quality & Treatment (WQT-18) on 22<sup>nd</sup> & 23<sup>rd</sup> March, 2018 Organized by Department of Chemistry, Directorate of Distance Education Madurai Kamaraj University Madurai 625 021 Tamil Nadu, India*

**Title: Synthesis and characterization of modified metal oxides for visible light assisted photo decoloration**

*N. Nagaganapathy, S. Pitchaimuthu and P. Velusamy*

2. *Two Day International Conference on Recent Trends In Chemistry and Biosciences (ICRTCB-2019) May 16 & 17, 2019 Organized by Department of Inorganic Chemistry, School of Chemistry, Madurai Kamaraj University Madurai 625 021 Tamil Nadu, India*

**Title : Photocatalytic behaviour of various metal oxides modified with  $\beta$ -cyclodextrin in visible light source**

Ponnusamy Velusamy and **Sakthivel Pitchaimuthu**

**Manuscript submitted to JOURNAL OF WATER CHEMISTRY AND TECHNOLOGY**

Photocatalytic decoloration of methylene blue dye in aqueous medium under visible light using TiO<sub>2</sub> and transition metals doped TiO<sub>2</sub> catalyst

**Manuscript under preparation for journal**

Synthesis and Characterization of CeZn<sub>2</sub>O<sub>4</sub> Nanospheres for Photocatalytic Decoloration of Brilliant Green Dye

## WORK DONE

### INTRODUCTION

Millions of various colored chemical substances have been generated within the last century or so, 10,000 of which are industrially produced. On a global scale, over 0.7 million tons of organic synthetic dyes are manufactured each year mainly for use in the textile, leather goods, industrial painting, food, plastics, cosmetics, and consumer electronic sectors. A sizable fraction of this is lost during the dyeing process and is released in the effluent water streams from the above industries. Therefore, decolorization and detoxification of organic dye effluents have taken an increasingly important environmental significance in recent years. As one of the most promising solutions for these problems, semiconductor photocatalysis has attracted much attention, since it is a “green” technology for decomposing water into hydrogen and oxygen, inactivating viruses and/or completely eliminating all kinds of contaminants, under the illumination of light under ambient conditions. To date, the TiO<sub>2</sub> semiconductor has undoubtedly proven to be one of the excellent photocatalysts for water splitting and the oxidative decomposition of many organic compounds. However, due to its wide band gap of 3.2 eV, TiO<sub>2</sub> can only be excited by ultraviolet or near ultraviolet radiation, which occupies only 4% of the incoming solar light spectrum on the earth. To efficiently utilize the visible region which covers the largest proportion of the solar spectrum, the development of visible light driven (VLD) photocatalysts is the current trend.

### AIM AND SCOPE OF THE WORK

The present work aims to utilize novel method to synthesis visible light driven photocatalyst of nanoheterostructures using hydrothermal/solvothermal method.

Photocatalysts will be synthesized with coupled Nano composite using suitable method. In order to harvest visible light either Natural or synthetic dyes will be utilized to study the photocatalytic activity of prepared catalysts. The photo catalytic efficiency will be studied.

## **EXPERIMENTAL PART:**

### **Reagents:**

All the chemicals used in the present study were of high purity, commercially available Analar grade (Merck, India). Doubly deionized water was used to carry out all the processes throughout the synthesis. Zinc nitrate hexahydrate, Nickel nitrate, Ferric ammonium nitrate and Copper Nitrate trihydrate, NaOH, HCl and Glycerol.

### **Preparation of modified-ZnO heterostructures:**

In a typical preparation, 0.2M of each metal nitrate was dispersed in 25 ml water and the drop wise addition of 0.3M sodium hydroxide, achieved pH range 5.8. This mixture was stirred and refluxed for 4h at 60°C, resulting in the formation of modified-ZnO. The precipitate thus obtained was separated from the reaction mixture and washed with deionised water to remove the adhering impurities and finally washed with glycerol for good morphology. It was then dried at oven and calcinated 250°C for 3hours.

### **Photoreactor :**

These reactors are among the most efficient for photochemical reactions since the lamps are effectively surrounded by the solution to be irradiated. The lamps are contained in double-walled immersion wells made of quartz, allowing water cooling and/or filtering of excitation radiation. Various flask designs enable reactions to be conducted under anaerobic conditions at low or constant temperature. These are double-walled vessels made of quartz glass which house the irradiation lamp. Inlet and outlet tubes provide for air or water cooling. A space between the walls allows filtering of certain wavelengths with liquids such as cobalt, nickel, copper sulphate, sodium nitrate solutions or gas such as chlorine to reduce secondary photochemical reactions of products.

The synthesized photocatalysts will be characterized utilizing the following instrumental techniques.

- ❖ SEM with EDS
- ❖ UV-DRS(ULTRA VIOLET DIFFUSED REFLECTANCE SPECTROSCOPY)
- ❖ X-RAY DIFFERATION (POWDER-XRD)

## RESULT AND DISCUSSION:

### CHARACTERIZATION:

#### UV-DRS:

The DRS of the as-prepared samples is shown in Fig.1. ZnO nanoparticles have strong absorption peaks at 365nm at visible light region. The observed red shift in ZnO-Cu 5% and ZnO-Cu 7% nanoparticles can be attributed to the electron-hole transition between ZnO and Cu. The above result indicates that dispersing ZnO on the Cu surface leads to the enhanced absorption in the visible light range, therefore, these ZnO-Cu nanoparticle would be promising for photocatalysis application. The enhanced light absorption may lead to forming more electron-hole pairs. The optical energy band gap of the nanoparticle was measured using the Tauc relation. Abruptly, similar UV-vis absorption curves were observed and the absorption edges were calculated using the formula

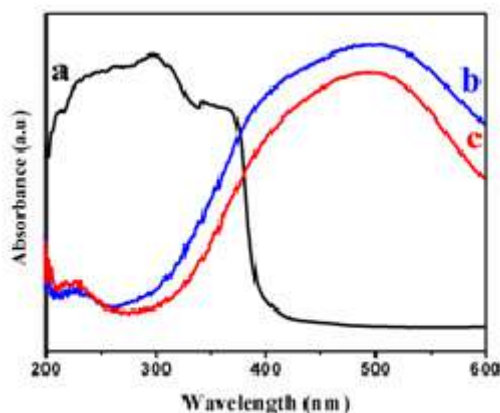


**Fig:1 DRS of the as-prepared samples (a = ZnO, b = 5% Cu-ZnO and c = 7% Cu-ZnO)**

$$\alpha h\nu = A (h\nu - E_g)^{n/2} \quad \text{----- (1)}$$

Where,  $\alpha$ ,  $h$ ,  $\nu$ ,  $A$ ,  $E_g$  are the absorption coefficient, Planck's constant, incident light frequency, proportionality constant, and band gap energy respectively. The obtained band gap energy values of ZnO, ZnO-Cu 5% and ZnO-Cu 7% are found to be 3.23eV, 2.08eV and 2.25eV respectively and it is displayed in Fig.2.

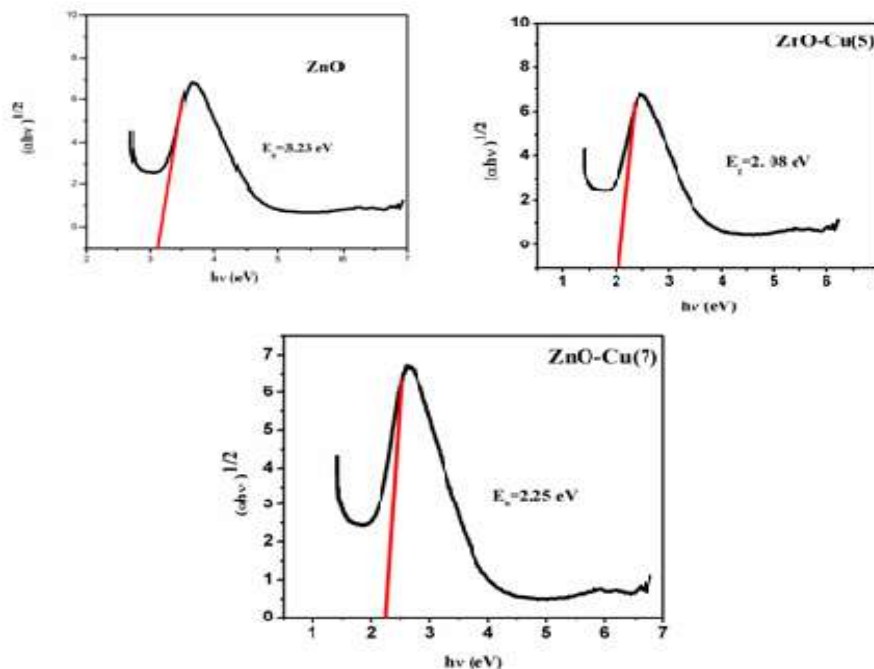


**Fig:2 Band gap energy for the particles**

Using the DRS results, the band edge positions of the nanocomposites were calculated theoretically using Mulliken electronegativity theory following the empirical equations 3 and 4.

$$E_{VB} = X - E_c + 0.5 E_g \quad \text{----- (2)}$$

$$E_{CB} = E_{VB} - E_g \quad \text{----- (3)}$$

Where  $E_{VB}$  is the valence band edge potential,  $E_{CB}$  is the conduction band edge potential,  $E_g$  is the band gap energy of the semiconductor,  $E_c$  is the scale factor of the hydrogen reference electrode (-4.5 eV), and  $\chi$  is the absolute electronegativity of the semiconductor, which is defined as the geometric mean of the absolute electronegativities of the constituent atoms. The calculated band edge potentials of the CB and VB of ZnO as given in Table 1.

**Table. 1. Estimated band-gap energies ( $E_g$ ) and calculated  $E_{VB}$  and  $E_{CB}$  of ZnO.**

Catalyst	Absolute electronegativity X(eV)	Calculated conduction band position $E_{VB}$ (eV)	Calculated valence band position $E_{CB}$ (eV)	Energy band gap $E_g$ (eV)
ZnO	5.80	2.915	-0.315	3.23

## XRD:

Figure.3: shows the X-ray powder diffraction patterns of ZnO, CuO, ZnO-Cu(5%), ZnO-Cu(7%) and ZnO-Cu(9%) particles. All the diffraction peaks of the samples can be indexed as the wurtzite structured hexagonal ZnO with lattice (JCPDS, No.36-1451), which indicate that the sample ZnO is in pure form. The high intensities of the XRD peaks of the sample suggest that the ZnO phase used in this work is highly crystalline. Diffraction peaks at  $31.73^\circ$ ,  $34.45^\circ$ ,  $36.28^\circ$ ,  $47.51^\circ$  and  $56.68^\circ$  correspond to (100), (002), (101), (102) and (110), planes of ZnO respectively. These XRD patterns give the monoclinic structure of CuO in agreement with the literature (JCPDS card no 45-0937), which indicates that the sample CuO is in pure form. Diffraction peaks at  $32.4^\circ$ ,  $35.1^\circ$ ,  $38.2^\circ$ ,  $48.7^\circ$ ,  $51.3^\circ$ ,  $58.0^\circ$ ,  $62.6^\circ$ ,  $66.83^\circ$  and  $68.13^\circ$  correspond to (110), (002), (111), (202), (020) and (202) planes of CuO respectively.

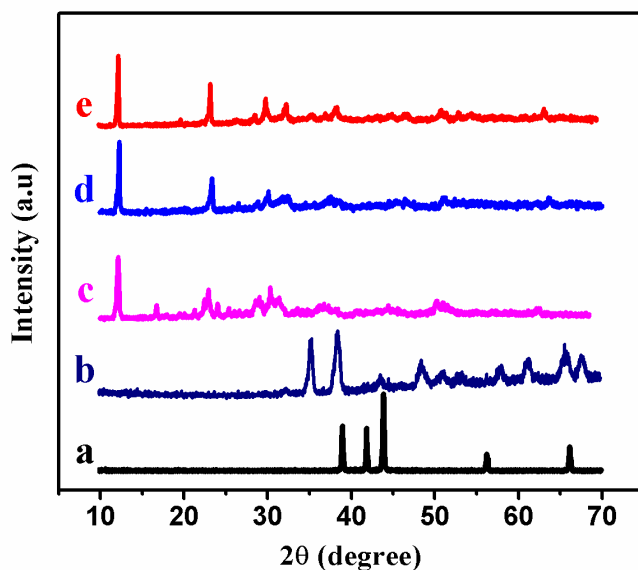


**Fig: 3** Xrd patterns of a) ZnO, b) CuO, c) ZnO-Cu(5%), d) ZnO-Cu(7%), e) ZnO-Cu(9%)  
**Morphological Studies: (SEM with EDS)**

The scanning electron microscopy (SEM) images of pure and Cu doped ZnO. The SEM micrograph indicates that the shape and morphology of ZnO nanoparticles changes with increasing Cu concentration. These images revealed that the individual particles were composed by the collection of particles of various shapes with increasing Cu concentration. This indicates that doping of Cu ions influences strongly on morphology of ZnO nanoparticles. These images



also show that the agglomeration in nanoparticles increases with increasing Cu concentration and dispersivity, homogeneity of particles was not good. This kind of structure can provide a better adsorption environment and more active site for the photocatalytic reaction. In this Fig 4: [A] CuO have the sphere structure,[B] indicates as RICEROD structure from (5%)Cu doped ZnO. [C] indicates FLAKES like structure increasing of Cu percentage(7%) [D] indicates PLATE like structure in coupled formation.

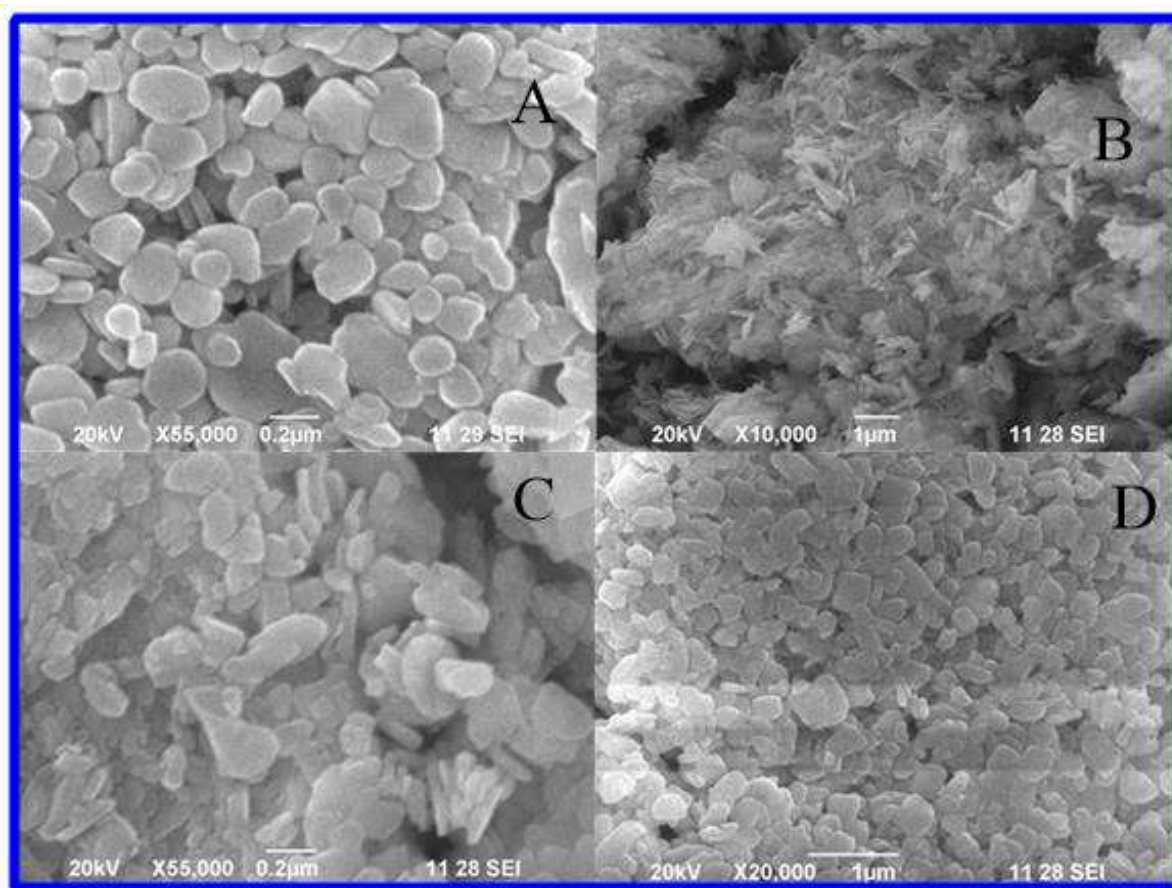


**(Fig:4) SEM images of A) CuO, B)ZnO-Cu(5%), C)ZnO-Cu(7%) and D)Coupling.**

Fig:5 The EDS shows the presents of element such as Zn, Cu, O, Cu-ZnO.

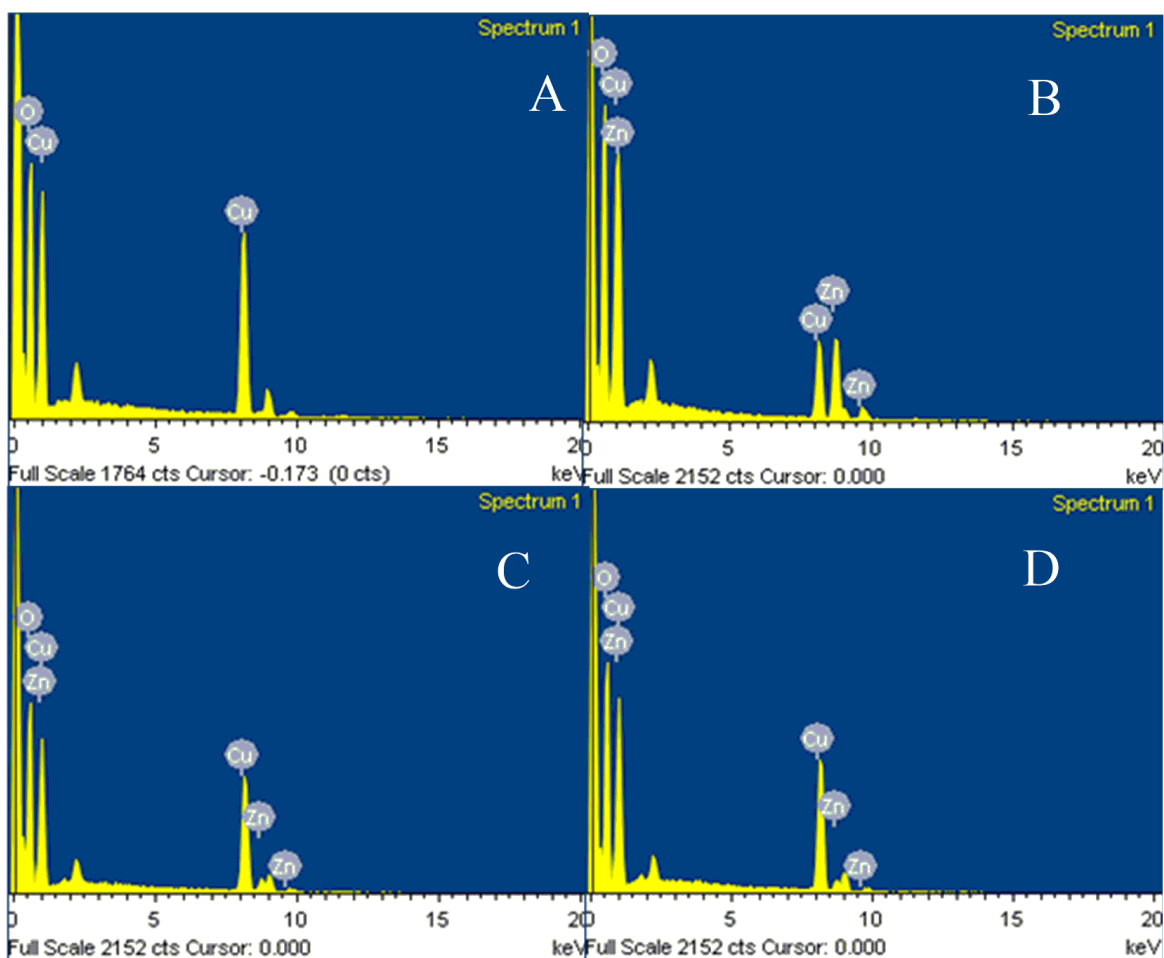


Fig:5 EDS images of the prepared Cu modified ZnO

### Photocatalytic Degradation:

The photodegradation was monitored by examining the variations in maximal absorption with respect to irradiation time in UV-Vis spectra. The photocatalytic activity of ZnO-Cu nanoparticle was investigated by measuring the degradation of GV at pH 6.5 in the presence of 1.0g/L catalyst **Fig.6**. From these experiments, it was observed that the concentration of GV photodegradation under visible light irradiation in the absence of the photocatalytic materials. The control experiments were performed for 30 min under the dark condition in the presence of photocatalytic materials, which indicated the absorption of dye on the active sites of the synthesized photocatalysts with the increase of irradiation time, the absorption peak at  $\lambda_{\max}$  645nm decreased gradually and after 180 min of irradiation. The photocatalytic degradation of EY in aqueous solution in the presence of ZnO-Cu resulting in 90% degradation efficiency. No

new absorption bands appeared, either in the visible and ultra-violet regions indicating the destruction of the conjugated structure.

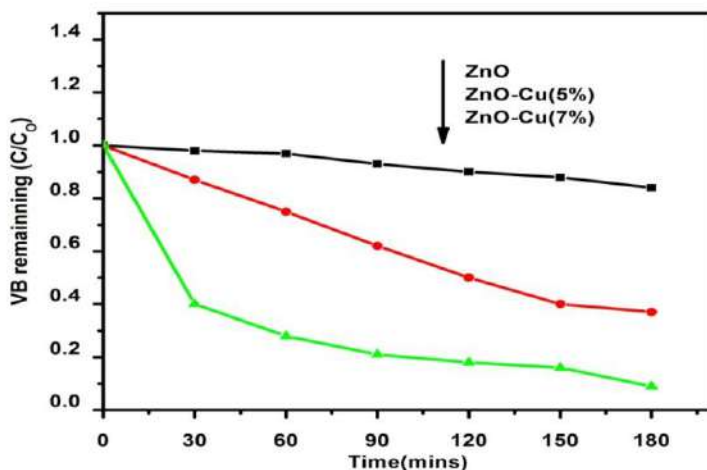


Fig:6 Photocatalyst degradation of Nanoparticle

## SUMMARY

In this work, a detailed study of the effect of nanoheterostructures of semiconductor catalyst on the photodegradation of GV dye has been carried out. XRD analyses reveal that ZnO and CuO conserved their Wurtzite crystal features and monoclinic lattices respectively during the irradiation. UV-Vis DRS demonstrated that Cu modification leads to a significant effect on the optical characteristics of ZnO. Cu/ZnO system has higher absorption intensity in the visible region compared to the ZnO catalyst systems.

Hence photodecoloration of dyes in Cu/ZnO systems exhibits better photocatalytic decoloration efficiency than that of all other catalyst systems. This work provides basic information on the promotion effects of Cu modification on the photodegradability of ZnO on dye in aqueous solution.

Comparing the results obtained from all the preliminary operational parameters discussed above, it is observed that, Cu/ZnO systems exhibit better photocatalytic decoloration efficiency than that of ZnO catalyst systems. Effect of modification of catalyst through Cu modification on ZnO in GV dye photodecoloration would probably leads to a high efficiency and selectivity than that of photodecoloration of dyes using ZnO as catalyst.

# SYNTHESIS AND CHARACTERIZATION OF CeZn<sub>2</sub>O<sub>4</sub> NANOSPHERES FOR PHOTOCATALYTIC DECOLORATION OF BRILLIANT GREEN DYE

## Abstract

CeZn<sub>2</sub>O<sub>4</sub> nanosphere photocatalysts have been successfully synthesized using a mixing annealing method. The synthesized composites exhibited significantly higher photocatalytic activity than a naked semiconductor in the photodegradation of Brilliant Green (BG) under visible light irradiation. The various operational parameters such as initial concentration, pH, irradiation time, amount of catalyst on photocatalytic activity were also investigated. The origin of the high level of activity was discussed based on the results of scanning electron microscopy, X-ray diffraction, UV–vis diffuse reflection spectroscopy. The enhanced activity of the catalysts was mainly attributed to the synergetic effect between the two semiconductors, the band potential of which matched suitably.

## Keywords

Photocatalysis, CeZn<sub>2</sub>O<sub>4</sub>, Brilliant Green

## Introduction

In recent years, a sizeable quantity of interest in photocatalysis has been focused on the photodegradation of organic pollutants through nanoscale semiconductor powders. Photocatalytic reactions using metal oxide semiconductor powders such as TiO<sub>2</sub>, ZnO, Fe<sub>2</sub>O<sub>3</sub>, ZrO<sub>2</sub>, and CeO<sub>2</sub> have received much attention because of possible practical applications. These metal oxides have been used for the decomposition of water to hydrogen and oxygen. They have

also been used for a wide range of chemical redox reactions such as the mineralization of organic pollutants in wastewater.

ZnO, as a well-known wide direct band gap ( $E_g=3.37\text{eV}$  at 300 K) semiconductor, has attracted much attention in recent years [1,2] for its potential application in environment improvements. Various kinds of ZnO nanostructures, such as nanoparticle, hollow sphere have been prepared for many applications [3–5]. Especially, due to the large aspect ratios of fibers, ZnO nanofiber and its based composite nanofibers, including ZnO–SnO<sub>2</sub>, TiO<sub>2</sub>–ZnO and Ag–ZnO composite nanofibers, have revealed superior photocatalytic activity than other types, and have been mainly used as photocatalyst to degrade dye pollutants [6–8].

Ceria (CeO<sub>2</sub>), as a fascinating rare earth material, has attracted much attention due to its applications in catalysis and chemical materials [9,10]. Accordingly, it was interesting to prepare CeO<sub>2</sub>–ZnO composites, and various efforts have been extensively developed. He et al. reported the CeO<sub>2</sub>–ZnO microspheres prepared by combining homogeneous precipitation with micro-emulsion, revealing high catalytic activity for the oxidative coupling of methane [11]. Mishra *et al.* prepared nanoparticle catalysts of CeO<sub>2</sub>–ZnO composites by amorphous citrate method, and they found that the presence of ceria in the composite oxide could enhance the catalytic activity for both cyclohexanol dehydrogenation and hydrogen transfer reactions [12]. However, due to the problems of aggregation and difficulties in recovery, these nanostructures might decrease the catalytic efficiency or even re-pollute the treated water or air [13].

It is reported that, the properties of CeO<sub>2</sub> are similar to the titania features such as wide band gap, nontoxicity, and high stability [14]. Because of its unique 4f electron configuration, CeO<sub>2</sub> has been frequently selected as a component to prepare complex oxides or as a dopant to improve titania-based catalysts. It is recently reported the photocatalytic behaviors of CeO<sub>2</sub> and

its modified catalyst under various irradiation to degrade dyes and antimicrobial activity [15-18].

Cerium oxide ( $\text{CeO}_2$ ) is an additive in the automotive three-way catalysts [19]. The redox couple of  $\text{Ce}^{3+}/\text{Ce}^{4+}$  and the high capacity to store oxygen of  $\text{CeO}_2$  have gained additional importance in the application of heterogeneous catalysis. However the poor thermostability of pure  $\text{CeO}_2$  has limited its application in oxygen storage [20, 21]. To overcome this problem, some strategies have been adopted like mixing with metal or metal oxide to increase the thermal stability. The mixing of two different metal oxides leads to not only the thermal stability but also the different physical and chemical property from the individual metal oxides [22].

Generally, hybrid photocatalysts show improved performance compared to their respective individual components [23, 24]. The achievement of visible-light photocatalysis depends on the prevention of electron-hole recombination [25-27]. Therefore, a number of efforts have been attracted to inhibit the recombination of electron-hole pairs and improve charge transport *via* coupling the wide band gap semiconductor photocatalysts with other materials such as metal or nonmetals doped ZnO (Fe, Au, Ag, Mn, or F, N, S and etc.,) composite, polymer modified ZnO composite, carbon nanotube (CNTs) or graphene –ZnO composites,  $\beta$ -CD modified ZnO [17, 23-30].

Among the different reported composites, the simplest and most viable composites are those that comprise different semiconductors, such as ZnO/CdO [13], ZnO/ $\text{Mn}_2\text{O}_3$  [15], and ZnO/ $\text{CeO}_2$  [16]. These are reported that ZnO combined with different semiconductors can effectively inhibit electron-hole recombination, and the resulting composite enabled the

degradation of pollutants to be extended from the UV to the visible light range because of the synergetic effect between these two semiconductors [28].

In this work, we fabricate and characterized the  $\text{CeZn}_2\text{O}_4$  nanospheres and their photocatalytic activity towards decoloration of BG dye and under visible light radiation have been studied and the results are documented. The optical property was tuned by changing the stoichiometric amount of  $\text{CeO}_2$  and calcination temperature and achieved longer wavelength adsorption in UV-Vis spectrum. The morphology and crystalline nature of the composites were characterized using FESEM and XRD techniques, respectively. The photocatalytic degradation of BG under visible light irradiation using the composite catalysts was investigated under various experimental conditions and the rate constant was calculated using pseudo first order kinetic model. A suitable mechanism has also been proposed to explain the photocatalytic activity of  $\text{CeO}_2$ .

## Materials

The commercial organic dye Brilliant Green (BG) (C.I. 42040;  $\lambda_{\text{max}} = 623 \text{ nm}$ ) was used as such. The semiconductor photocatalyst  $\text{Ce}(\text{NO}_3)_2 \cdot 6\text{H}_2\text{O}$  and  $\text{Zn}(\text{NO}_3)_2 \cdot 6\text{H}_2\text{O}$  were purchased from Merck Chemicals. 2-methylimidazole and all other chemicals were of the Analytical grade, received used without further purification. Double distilled water was used throughout this study for the preparation of all the experimental solutions.

## Experimental Methods

In a typical synthesis process, the 1:2 molar ratio of  $\text{Ce}(\text{NO}_3)_2 \cdot 6\text{H}_2\text{O}$  and  $\text{Zn}(\text{NO}_3)_2 \cdot 6\text{H}_2\text{O}$  were dissolved in 30 mL of methanol to form a clear homogenous solution, which was subsequently poured into 10 mL of MeOH containing 12 mmol of 2-methylimidazole. The resulting mixed solution was initially stirred for 5 minutes to ensure

complete mixing of reactants then incubated for 24h at room temperature. As formed yellow coloured Zeolitic Imidazolate Frame work (Ce-ZIF) of Ce-Zn was centrifuged and washed several times with ethanol. The final product was calcined in tube furnace at different temperatures at 400°C and 600°C for three hours with the heating ramp of 5 °C min<sup>-1</sup> under the nitrogen protection. Finally, the yellow colour of Zeolitic Imidazolate Frame work (ZIF) of Ce-Zn changed into black coloured free flowing powder and designated as CeZn<sub>2</sub>O<sub>4</sub>.

### **Photocatalytic Activity**

The photocatalytic activities of the ZnO and synthesized CeZn<sub>2</sub>O<sub>4</sub> nanocomposite were investigated for the photodegradation by choosing BG as model substrate under visible light irradiation. The photo reactor “Heber Visible Annular Type Photo reactor” (Model No HIPR-MP400) equipped with 300W tungsten halogen lamp (8500 lumen) was used for the investigation. The photo reactor was comprised of a borosilicate immersion jacketed tube to hold the lamp with inlet and outlet for water circulation to cancel the IR radiation. The immersion well is held at the centre of a reaction chamber. The inner surface of reaction chamber is fitted with highly polished anodized aluminum reflector. In a typical process, aqueous suspension of BG and composite was taken in a glass tube. Prior to irradiation, the suspension was magnetically stirred in dark for 30min to attain the adsorption-desorption equilibrium. At the given time interval 3.5mL of the sample was withdrawn and centrifuged to separate the filtrate for analysis. The degradation of BG was determined by measuring the absorbance at 623 nm on UV-Visible Spectrophotometer.



## Results and discussion

The formation of bimetallic ZIFs with a unique nanosphere morphology was first achieved by the reaction of 2-methylimidazole with divalent  $\text{Zn}^{2+}$  ions and tetravalent Ce ions in methanol solution at room temperature ambient pressure.

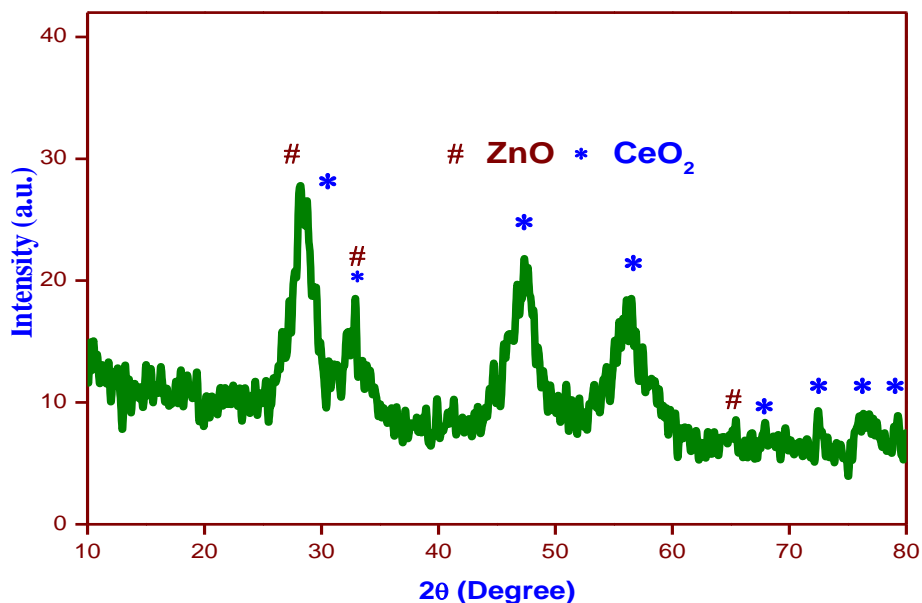


**Figure 1.** XRD pattern for as calcined  $\text{CeZn}_2\text{O}_4$ -nanospheres .

The crystallinity of  $\text{CeZn}_2\text{O}_4$ -n was examined in X-ray diffraction (XRD) as shown in Figure 1. All Zn-Ce-ZIFs-*n* exhibit strong diffraction peaks at similar positions and all peaks match well with the simulated ZIF-8, indicating that they have high crystallinity and pure-phase ZIF-8 structure. Crystal structure and crystallinity of the  $\text{CeZn}_2\text{O}_4$  nanostructures were corroborated by XRD which is represented in Fig. 2. The strong diffraction peaks of  $\text{CeO}_2$  and ZnO are detected in the sample, those marked with "\*" could be indexed to (111), (200), (220), (311), (222), (400), (331), (420), and (422) phases, which demonstrate that the synthesized product have well-crystalline distinct cubic fluorite structure of  $\text{CeO}_2$ . Besides, the feature peak marked with "#" are indexed to wurtzite hexagonal phase ZnO (JCPDS 36-1451) [31-33]. All the

characteristic peaks observed are well-matched with those of cubic fluorite  $\text{CeO}_2$  and wurtzite hexagonal well-crystalline  $\text{ZnO}$ . XRD thus confirms that the obtained nanomaterial is the

combination of  $\text{CeZn}_2\text{O}_4$ .

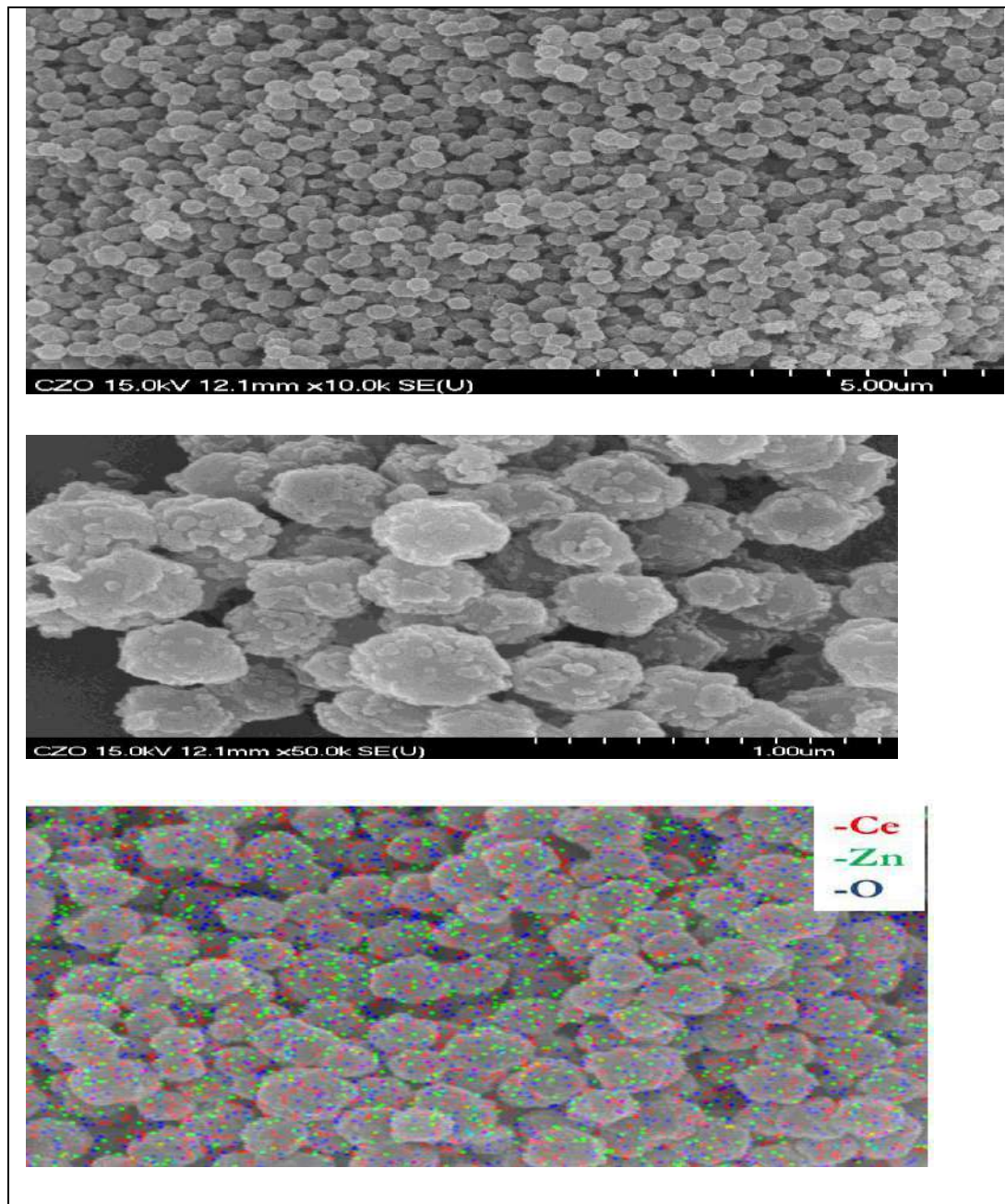


**Figure 2,** SEM images and elemental mapping for  $\text{CeZn}_2\text{O}_4$  nanospheres

The morphology of the  $\text{CeZn}_2\text{O}_4$ -

“n” were characterized by field-emission scanning electron microscopy (FESEM), and the representative FESEM images of  $\text{CeZn}_2\text{O}_4$ -“n” are shown in Figure 2 (a-c). It can be clearly

observed from the FESEM images that as formed  $\text{CeZn}_2\text{O}_4$  are nanospheres and all spheres has good uniform diameter size of about 0.4 micron. The high resolution FESEM image shown in Figure 2c reveals that these particles have spherical geometry, and each of them is an irregular nanospheres crystal with very rough surface. The presence of rough surface on the irregular nanospheres may enhance the water treatment process due to increment in the active surface area than the uniform surface. To ensure the uniform distribution of  $\text{CeZn}_2\text{O}_4$  nanospheres, the elemental mapping was conducted and presented as figure 2c, the elemental mapping study suggest that the  $\text{CeZn}_2\text{O}_4$  is uniformly formed.

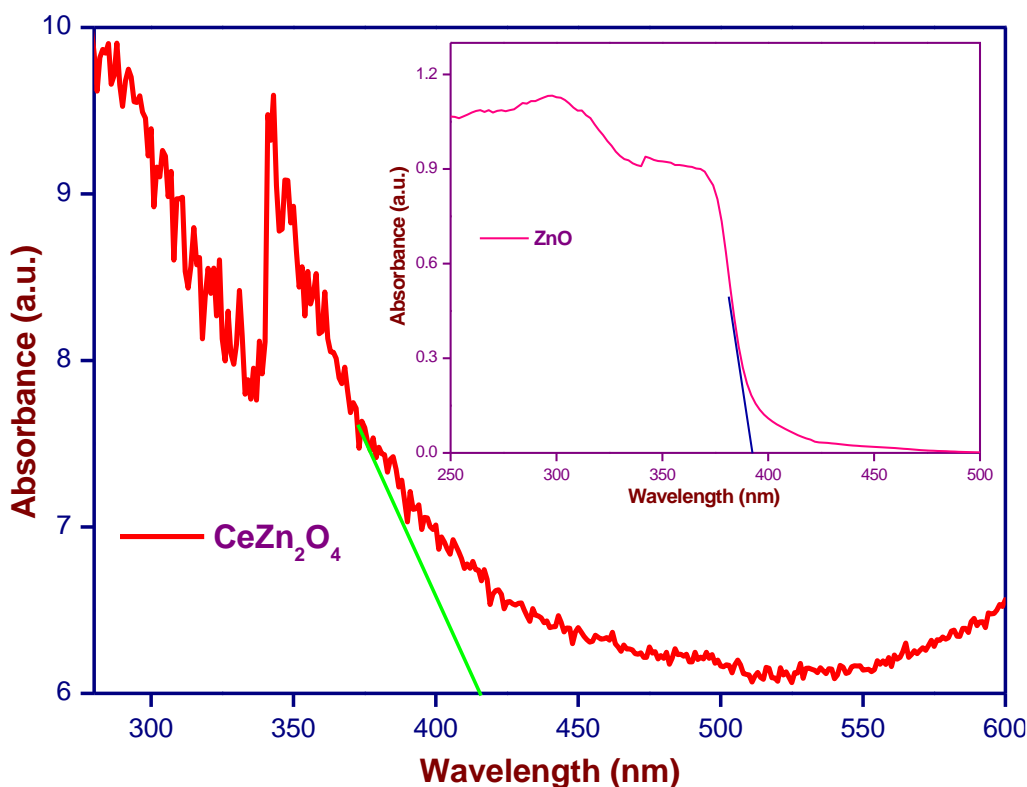


**Figure 3.** UV-DRS spectra of  $\text{CeZn}_2\text{O}_4$  nanospheres (Absorbance vs Wavelength)

The estimation of the optical absorption wavelength of the prepared nanocomposites is an essential factor because, during photocatalysis, adequate electrons will be excited from the valence band to the conduction band of the photocatalysts only if the energy of the incident light

is equivalent to or greater than the photocatalysts' band-gap energy. Otherwise, the photocatalytic activity will be limited or not occur. Therefore, we measured the optical absorption wavelength of  $\text{CeZn}_2\text{O}_4$  nanocomposites a UV-vis spectrophotometer; the results are shown in Fig. 3 and Fig 4.

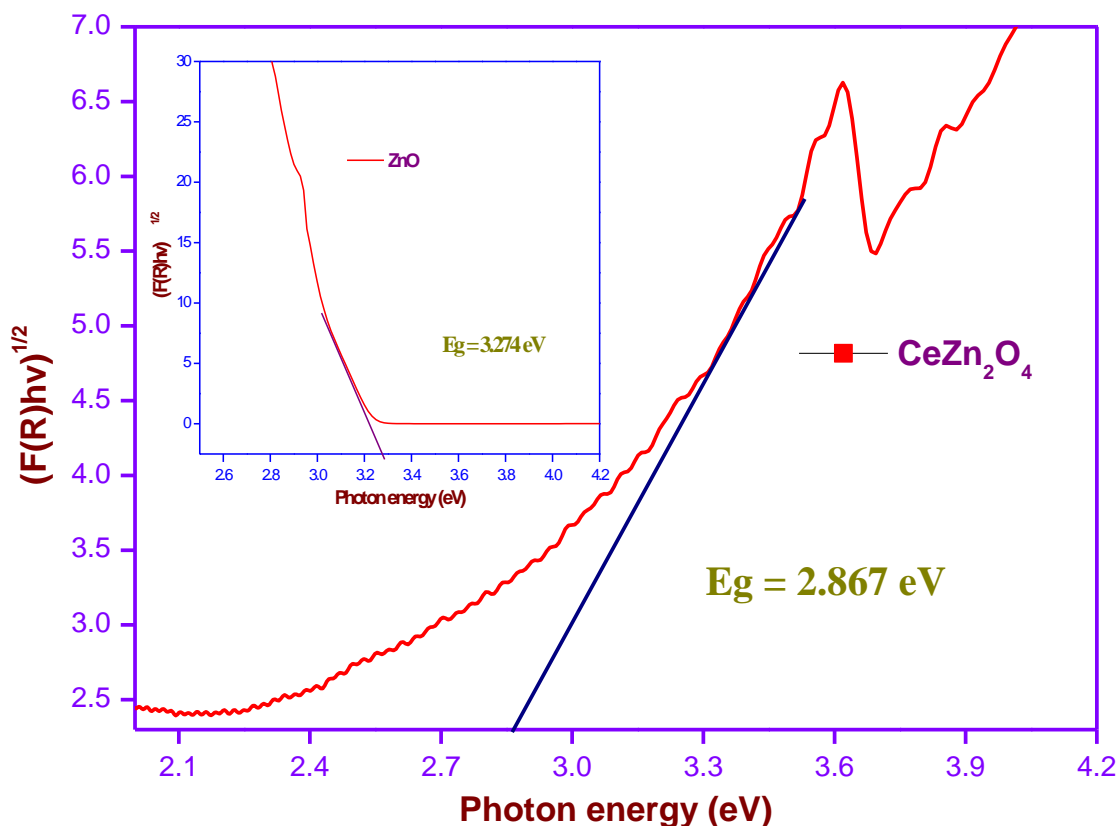


**Figure 4.** UV-DRS spectra of ZnO and  $\text{CeZn}_2\text{O}_4$  ( $(F(R)hv)^{1/2}$  vs Photon energy)

The absorption edge of the pure ZnO lies in the blue region; the corresponding wavelengths are  $\sim 392$  nm (3.274 eV), which lie in the UV region. Conversely,  $\text{CeZn}_2\text{O}_4$  nanocomposite (red shift) absorbance over a wider range (at wavelengths greater than 415 nm), which led to a shift toward the red region of the spectrum, as highlighted in Figure 3. The band

edge of the  $\text{CeZn}_2\text{O}_4$  nanocomposite is 2.867 eV (Figure 4) because it contains amorphous  $\text{CeZn}_2\text{O}_4$ , whereas the pure  $\text{ZnO}$  has a very sharp band edge [34]. This wider band edge for amorphous  $\text{CeZn}_2\text{O}_4$  has been speculated to arise from the formation of  $\text{Ce}^{4+}$  ions that have induced some localized mid-gap states in the band gap [35,36]. Therefore, the UV-Vis absorption results confirm that the nanocomposite can harvest visible light and generate a greater number of electrons and holes under visible-light irradiation<sup>15</sup>. These results also suggest that, during the photocatalytic reactions, the generated holes and electrons could actively participate in oxidation and reduction reactions [28, 37].

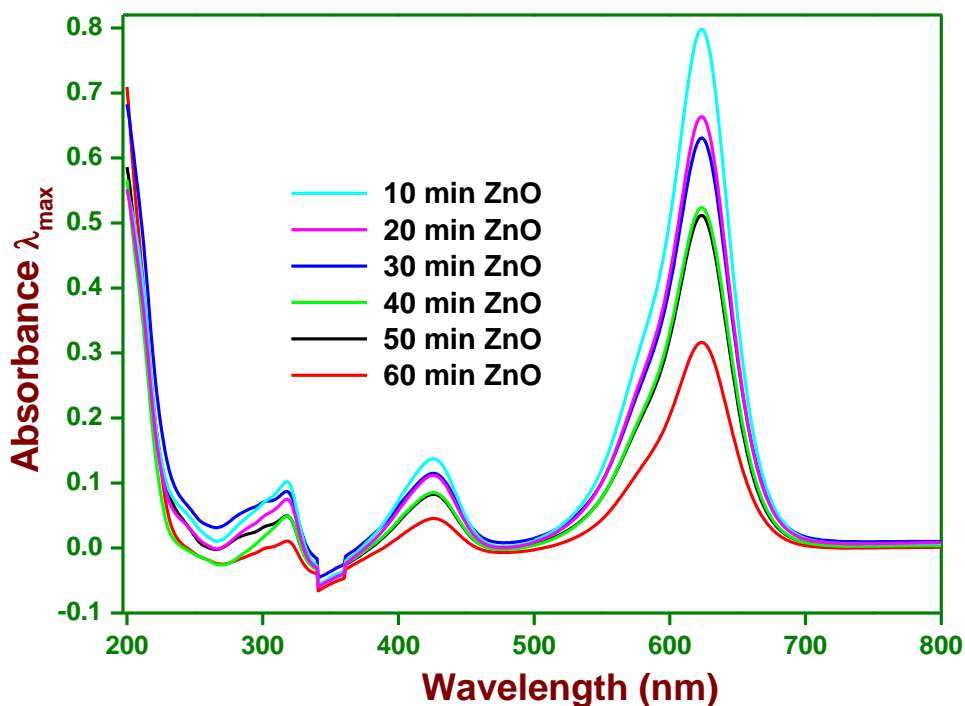


**Figure 5.** Time dependent absorption spectrum for the degradation of BG dye by  $\text{ZnO}$

## Photocatalytic Activity

Photocatalytic activities of ZnO and CeZn<sub>2</sub>O<sub>4</sub> nanospheres have been investigated under visible light irradiation. The photocatalytic activity at 0.5 g/L of ZnO or CeZn<sub>2</sub>O<sub>4</sub> nanospheres and 20mg/L of BG dye concentration was shown in Figure 5 and 6. The CeZn<sub>2</sub>O<sub>4</sub> nanospheres shows high photocatalytic activity.

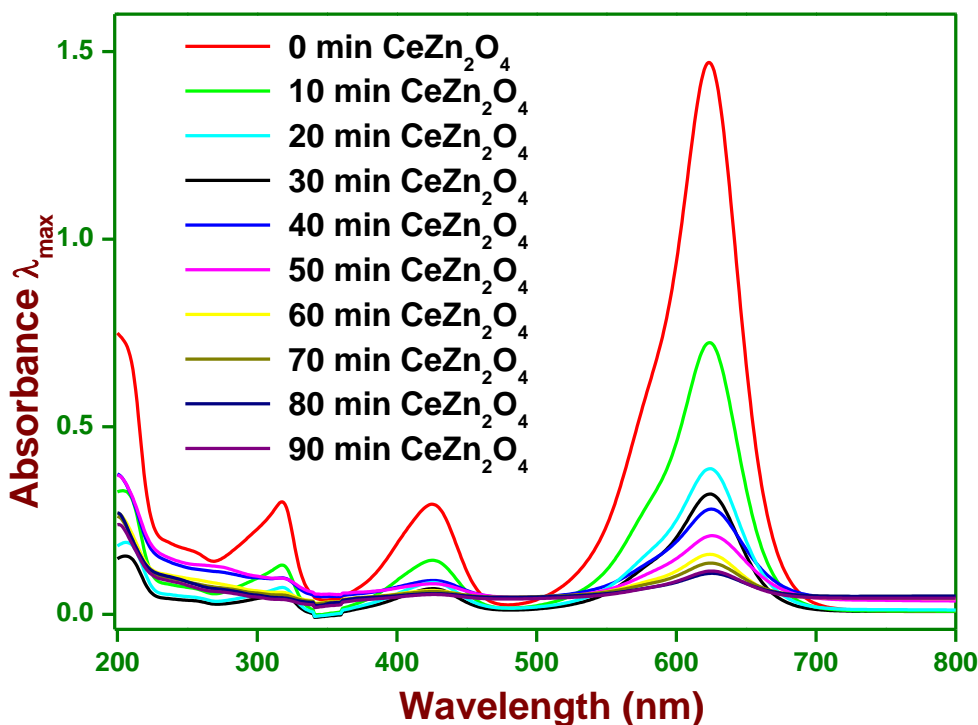


**Figure 6.** Time dependent absorption spectrum for the degradation of BG dye by CeZn<sub>2</sub>O<sub>4</sub> nanospheres

The illumination time was varied from 10 min. to 90 min. The remaining concentration of BG dye is decreased with an increase the illumination time. It is observed that nearly 98.8 % decoloration of BG dye for CeZn<sub>2</sub>O<sub>4</sub> is achieved with in 80 min (Figure 7). But ZnO catalyst systems have lower percentage removal than that of CeZn<sub>2</sub>O<sub>4</sub> system. This is due to the band gap of the catalyst decreased from 3.274 eV to 2.867 eV, the photocatalytic activity is increased.

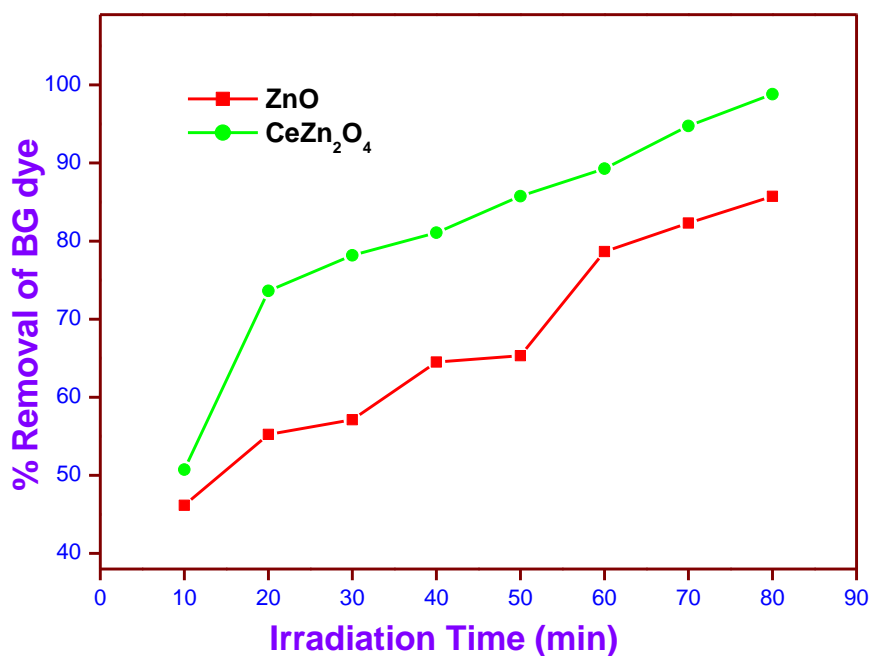


Figure 7. Photocatalytic degradation of BG dye by ZnO and CeZn<sub>2</sub>O<sub>4</sub> nanospheres

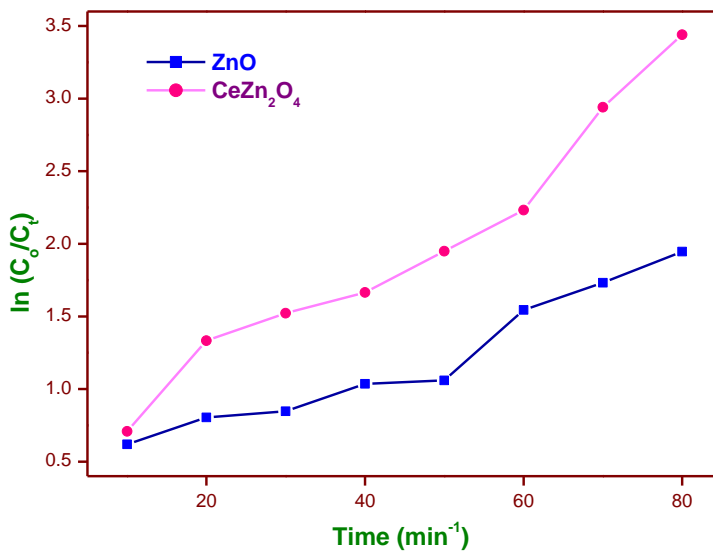


Figure 8. Kinetic profile for the degradation of BG

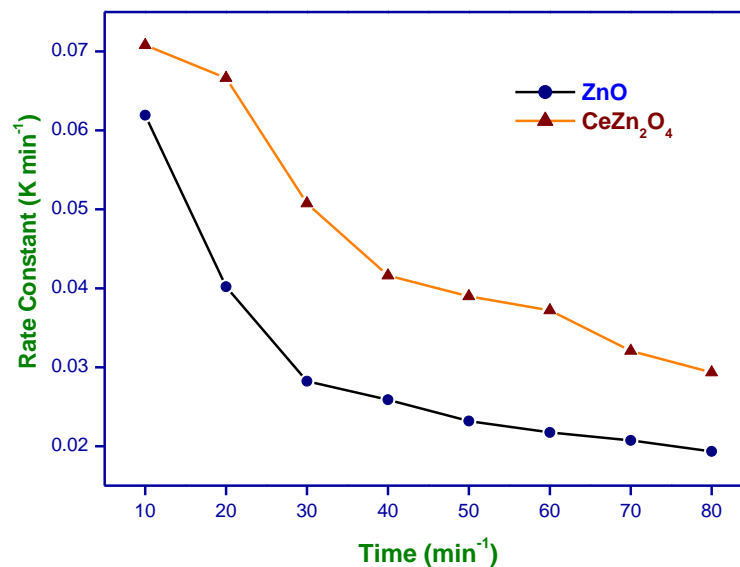


Figure 9. Rate constant promotion of BG

Photocatalytic degradation of many organic dyes follows a pseudo first order Langmuir-Hinshelwood kinetic model. The rate of the reaction is calculated by plotting  $\ln(C_0/C_t)$  versus irradiation time using the following equation [29,30]:

$$\ln(C_0/C_t) = k_{app}t$$

Where  $C_0$  is the initial concentration of the BG dye solution,  $C_t$  is the concentration of the BG dye solution at time  $t$ , and  $k$  is the rate constant ( $\text{min}^{-1}$ ). The kinetic profiles for the degradation of BG shows in Figure 8 and the calculated rate constants are given in Figure 9.

From the observed results, it is clearly understood that the high degradation rate was observed for  $\text{CeZn}_2\text{O}_4$  and the rate of the reaction is low for ZnO. This increase in the rate may be due to the low band gap of  $\text{CeZn}_2\text{O}_4$ . The promotion of photodecoloration rate of BG dye tends to increase in  $\text{CeZn}_2\text{O}_4/\text{Visible}$  light system than ZnO/Visible light system (Fig. 9). This suggests that the promotion of photodecoloration rate of BG dye here are due to increase of radicals generated by the  $\text{CeZn}_2\text{O}_4/\text{Visible}$  light system than ZnO/Visible light system.



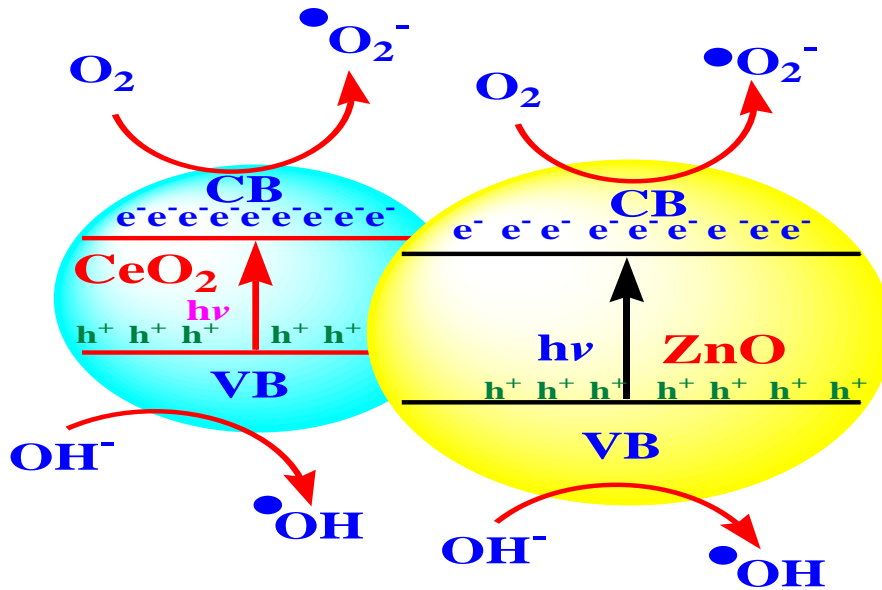


**Figure 9.** Proposed mechanism of  $\text{CeZn}_2\text{O}_4$

Fig. 10 represents the photocatalytic pathway mechanism for the  $\text{CeZn}_2\text{O}_4$  nanostructure under visible light irradiation. During the photocatalytic reaction, when the surface of the  $\text{CeZn}_2\text{O}_4$  is irradiated with visible light, electrons in the valence band of  $\text{CeO}_2$  are excited because of its small band gap [35]. The excited electrons are transferred to the conduction band of  $\text{ZnO}$ . The conduction band edge positions of  $\text{ZnO}$  and  $\text{CeO}_2$  are very close to each other. The injection of electrons from the conduction band of  $\text{ZnO}$  into conduction band of  $\text{CeO}_2$  nanoparticles is expected to retard the reverse reaction between the photogenerated charge carriers [26]

The conduction band electrons react with adsorbed oxygen molecules during the reaction process and get converted into superoxide anion. This superoxide anion reacts with water molecules and finally forms hydroxide radicals. These radicals effectively degrade the BG dye effluents under visible light irradiation. Moreover,  $\text{CeZn}_2\text{O}_4$  nanostructure photocatalyst having oxygen vacancies and  $\text{Ce}^{4+}$  due to line defect generates intermediate states which induce

narrowing of band gap which was confirmed by UV-DRS. Thus, oxygen vacancies and  $Ce^{4+}$  lead to improve the visible light induced photocatalytic degradation through harvesting maximum amount of visible light in short time. The similar statement has been reported by several other authors [37-42]. Therefore, we too assume that the  $CeZn_2O_4$  nanostructure shows excellent efficiency for the degradation of BG dye effluent owing to the  $Ce^{4+}$  and oxygen vacancies present in this system, which would be helpful to improve the photocatalytic activity of the  $CeZn_2O_4$  nanostructure under visible light irradiation.

## Conclusions

The  $CeZn_2O_4$  nanocomposites material have been prepared and characterized by FESEM, PXRD and UV-DRS analysis. The UV-DRS shows an increasing absorption in the visible region. The FESEM results were confirming the formation of  $CeZn_2O_4$  nanocomposites are nanospheres and all spheres has good uniform diameter size of about 0.4 micron. XRD thus confirms that the obtained nanomaterial is the combination of  $CeZn_2O_4$ . All the characteristic peaks observed are well-matched with those of cubic fluorite  $CeO_2$  and wurtzite hexagonal well-crystalline ZnO.  $CeZn_2O_4$ /Visible light system exhibited superior photocatalytic degradation of BG dye than that of ZnO/Visible light system. Therefore, because of its promising and enhanced photocatalytic degradation performance, this can be effectively used for future environmental applications.

## Acknowledgement

The authors thank the Management and the Principal of Thiagarajar College, Madurai, India for providing necessary facilities. Authors also thank the University Grants Commission, New Delhi, for the financial support through UGC-Minor Research Project Ref. [UGC - Ref. No.F. No. 6450/2016 (SR) Dated:30.06.2017].

## References

- [1] Y. Zhang, Y.H. Wen, J.C. Zheng, Z.Z. Zhu, [Strain-induced structural and direct-to-indirect band gap transition in ZnO nanotubes](#), Phys Lett A 374 (2010) 2846–9.
- [2] X.W. Sun, J.Z. Huang, J.X. Wang, Z. Xu, [A ZnO Nanorod Inorganic/Organic Heterostructure Light-Emitting Diode Emitting at 342 nm](#), Nano Lett 8 (2008) 1219–23.
- [3] W.J.E. Beek, M.M. Wienk, R.A. J. Janssen, Hybrid Solar Cells from Regioregular Polythiophene and ZnO Nanoparticles, Adv Funct Mater 16 (2006) 1112–6.
- [4] J. Zhang, S. Wang, Y. Wang, M. Xu, H. Xia, S. Zhang, et al. ZnO hollow spheres: Preparation, characterization, and gas sensing properties Sens Actuators B 139 (2009) 411–7.
- [5] Y. Zhang, Y. Liu, L. Wu, H. Li, L. Han, B. Wang, et al. Effect of annealing atmosphere on the photoluminescence of ZnO nanospheres, Appl Surf Sci 255 (2009) 4801–5.
- [6] X.D. Wang, C.J. Summers, Z.L. Wang, Large-Scale Hexagonal-Patterned Growth of Aligned ZnO Nanorods for Nano-optoelectronics and Nanosensor Arrays, Nano Lett 4 (2004) 423–6.
- [7] R. Liu, H. Ye, X. Xiong, H. Liu, Fabrication of TiO<sub>2</sub>/ZnO composite nanofibers by electrospinning and their photocatalytic property, Mater Chem Phys 121 (2010) 432–9.
- [8] D. Lin, H. Wu, R. Zhang, W. Pan, Enhanced Photocatalysis of Electrospun Ag–ZnO Heterostructured Nanofibers Chem Mater 21 (2009) 3479–84.
- [9] Cui MY, He JX, Lu NP, Zheng YY, Dong WJ, Tang WH, et al. Morphology and size control of cerium carbonate hydroxide and ceria micro/nanostructures by hydrothermal technology, Mater Chem Phys 121 (2010) 314–9.
- [10] Cui MY, Yao XQ, Dong WJ, Tsukamoto K, Li CR. Template-free synthesis of CuO–CeO<sub>2</sub> nanowires by hydrothermal technology, J Cryst Growth 2010;312:287–93.
- [11] He Y, Yang B, Cheng G. On the oxidative coupling of methane with carbon dioxide over CeO<sub>2</sub>/ZnO nanocatalysts, Catal Today 2004;98:595–600.
- [12] Mishra BG, Rao GR. Promoting effect of ceria on the physicochemical and catalytic properties of CeO<sub>2</sub>–ZnO composite oxide catalysts, J Mol Catal A Chem 2006;243:204–13.
- [13] Electrospinning of CeO<sub>2</sub>–ZnO composite nanofibers and their photocatalytic property, Chaorong Li, Rui Chen, Xiaoqiang Zhang, Shunxin Shu, Jie Xiong, Yingying Zheng, Wenjun Dong, Mater Lett 65 (2011) 1327–1330

- [14] Hu, S. Zhou, F. Wang, L. & Zhang, J. 2011 Preparation of Cu<sub>2</sub>O/CeO<sub>2</sub> heterojunction photocatalyst for the degradation of Acid Orange 7 under visible light irradiation, *Catal Comm* 12, 794–797.
- [15] Borker, P. & Salker, A.V. 2007 Solar assisted photocatalytic degradation of Naphthol Blue Black dye using Ce<sub>1-x</sub>Mn<sub>x</sub>O<sub>2</sub>, *Mater Chem Phys* 103 (2007) 366-370.
- [16] Zhai, Y.Q. Zhang, S.Y, Pang, H. 2007 Preparation, characterization and photocatalytic activity of CeO<sub>2</sub> nanocrystalline using ammonium bicarbonate as precipitant, *Mater Lett* 61 (2007) 1863-1866.
- [17] R. Saravanan, N. Karthikeyan, S. Govindan, V. Narayanan, A. Stephen, Photocatalytic degradation of organic dyes using ZnO/CeO<sub>2</sub> nanocomposite material under visible light, *Adv. Mater. Res.* 584 (2012) 381–385.
- [18] M.M. Khan, S.A. Ansari, J.H. Lee, M.O. Ansari, J. Lee, M.H. Cho, Electrochemically active biofilm assisted synthesis of Ag@CeO<sub>2</sub> nanocomposites for antimicrobial activity, photocatalysis and photoelectrodes, *J. Colloid Interface Sci.* 431 (2014) 255–263.

## Introduction

- [19] J.G.Nunan, H. J. Robota, M. J. Cohn, and S. A. Bradley, “Physicochemical properties of Ce-containing three-way catalysts and the effect of Ce on catalyst activity,” *Journal of Catalysis*, vol. 133, no. 2, pp. 309–324, 1992.
- [20] A. Laachir, V. Perrichon, A. Badri et al., “Reduction of CeO<sub>2</sub> by hydrogen. Magnetic susceptibility and Fourier-transform infrared, ultraviolet and X-ray photoelectron spectroscopy measurements,” *Journal of the Chemical Society, Faraday Transactions*, vol. 87, no. 10, pp. 1601–1609, 1991.
- [21] J. E. Kubsh, J. S. Rieck, and N. D. Spencer, “Cerium oxide stabilization: physical property and three-way activity considerations,” *Studies in Surface Science and Catalysis*, vol. 71, pp. 125–138, 1991.
- [22] S. Prabhu, T. Viswanathan, K. Jothivenkatachalam and K. Jeganathan, Visible Light Photocatalytic Activity of CeO<sub>2</sub>-ZnO-TiO<sub>2</sub> Composites for the Degradation of Rhodamine B, *Indian Journal of Materials Science* Volume 2014, <http://dx.doi.org/10.1155/2014/536123> .

- [23] Jiang, Y., Sun, Y., Liu, H., Zhu, F. & Yin, H. Solar photocatalytic decolorization of C.I. Basic Blue 41 in an aqueous suspension of TiO<sub>2</sub>-ZnO, *Dyes. Pigm.* **78**, 77 – 83 (2008).
- [24] Saravanan, R. *et al.* ZnO/Ag nanocomposite: an efficient catalyst for degradation studies of textile effluents under visible light, *Materials Science and Engineering C* **33**, 2235 – 2244 (2013).
- [25] Yu, Q. *et al.* Fabrication, structure, and photocatalytic activities of boron-doped ZnO nanorods hydrothermally grown on CVD diamond film, *Chem. Phys. Lett.* **539**, 74 – 78 (2012).
- [26] Saravanan, R., Shankar, H., Prakash, T., Narayanan.V. & Stephen, A. ZnO/CdO composite nanorods for photocatalytic degradation of methylene blue under visible light, *Mater. Chem. Phys.* **125**, 277 – 280 (2011).
- [27] Anandan, S., Ohashi, N. & Miyauchi, M. ZnO-based visible-light photocatalyst: Band-gap engineering and multi-electron reduction by co-catalyst, *Appl. Catal B: Environ.* **100**, 502 – 509 (2010).
- [28] Saravanan, R., Gupta, V. K. Narayanan, V. & Stephen, A. Visible light degradation of textile effluent using novel catalyst ZnO/ $\gamma$ -Mn<sub>2</sub>O<sub>3</sub>, *J. Taiwan Inst. Chem. Engrs.* **45**, 1910 – 1917 (2014).
- [29] S. Pitchaimuthu, S. Rajalakshmi, N. Kannan, P. Velusamy, Enhancement of zinc oxide-mediated solar light decoloration of Acid Yellow 99 dye by addition of  $\beta$ -CD, *Appl Water Sci* (2015) 5:201–208 DOI 10.1007/s13201-014-0181-y .
- [30] S. Pitchaimuthu, P. Velusamy, Modification of the photocatalytic performance of various metaloxides by the addition of  $\beta$ -cyclodextrin under visible light irradiation, *Journal of Water Process Engineering* xxx (2016) xxx–xxx, <http://dx.doi.org/10.1016/j.jwpe.2016.10.009>.
- [31] F. Niu, D. Zhang, L. Shi, X. He, H. Li, H. Mai and T. Yan: *Mater. Lett.*, 2009, 63, 2132.
- [32] F. Xu, G.H. Du, M. Halasa and B.L. Su: *Chem. Phys Lett.*, 2006, 426, 129.

- [33] M. Faisal, S.B. Khan, M.M. Rahman, A.Jamal, K. Akhtar and M.M. Abdullah, Role of ZnO-CeO<sub>2</sub> Nanostructures as a Photocatalyst and Chemi-sensor, *J. Mater. Sci. Technol.*, 2011, 27(7), 594-600.
- [34] Kang, Y. *et al.* An amorphous carbon nitride photocatalyst with greatly extended visible-light-responsive range for photocatalytic hydrogen generation, *Advanced Materials* **27**, 4572 – 4577 (2015).
- [35] Khan, M. M. et al. Defect-Induced Band Gap Narrowed CeO<sub>2</sub> Nanostructures for Visible Light Activities. *Industrial & Engineering Chemistry Research*, 53, 9754–9763 (2014).
- [36] Ansari, S. A., Khan, M. M., Ansari, M. O., Lee, J. & Cho, M. H., Band Gap Engineering of CeO<sub>2</sub> Nanostructure by Electrochemically Active Biofilm for Visible Light Applications. *RSC Advances* 4, 16782–16791 (2014).
- [37] Saravanan Rajendran<sup>1</sup>, Mohammad Mansoob Khan<sup>2</sup>, F. Gracia<sup>1</sup>, Jiaqian Qin<sup>3</sup>, Vinod Kumar Gupta<sup>4</sup> & Stephen Arumainathan<sup>5</sup> Ce<sup>3+</sup>-ion-induced visible-light photocatalytic degradation and electrochemical activity of ZnO/CeO<sub>2</sub> nanocomposite, *Scientific Reports* (2016) 6:31641 DOI: 10.1038/srep31641
- [38] Xu, Y. & Schoonen, M. A. A. The absolute energy positions of conduction and valence bands of selected semiconducting minerals, *Am. Mineral.* **85**, 543–556 (2000).
- [39] Aslam, M. *et al.* The effect of sunlight induced surface defects on the photocatalytic activity of nanosized CeO<sub>2</sub> for the degradation of phenol and its derivatives, *Appl. Catal B: Environ.* **180**, 391–402 (2016).
- [40] Saravanan, R. *et al.* ZnO/Ag/Mn<sub>2</sub>O<sub>3</sub> nanocomposite for visible light induced industrial textile effluent degradation, uric acid and ascorbic acid sensing and antimicrobial activity, *RSC Adv.* **5**, 34645–34651 (2015).
- [41] Yang, Y. *et al.* Photocatalysis: constructing a metallic/semiconducting TaB<sub>2</sub>/Ta<sub>2</sub>O<sub>5</sub> core/shell heterostructure for photocatalytic hydrogen evolution, *Advanced Energy Materials*, **4**, 1400057(1–7) (2014).

[42] Mohammad Hossein Habibi, Mosa Fakhrpor, Improved photo-catalytic activity of novel nano-dimension Ce/Zn composite oxides deposited on flat-glass surface for removal of Acid Black 4BN dye pollution, J Mater Sci: Mater Electron (2016) DOI 10.1007/s10854-016-5848-8

## ANNEXURE-I

### Report of the work done

Detailed literature survey has been carried out on the topics of redox reaction of organic molecules, dyes, inorganic compounds and metal ions by using the libraries of our College library and internet at Madurai Kamaraj University, Madurai, and required reprints were collected.

#### Photodegradation of dyes

After the literature survey, required equipments, chemicals and glasswares were purchased. The Objectives of the work is to synthesize metal oxide heterostructure nanocomposite with enhanced photocatalytic activity. In the presence study, metal oxide heterostructures like CeO<sub>2</sub>/ZnO, NiO/ZnO, CuO/ZnO have been synthesized. The photodegradation studies started with semiconductor photocatalysts on Gentian Violet (GV) dye under visible light source.

The degradation of GV dye were studied by photodegradation technique with prepared semiconductor photocatalyst *i.e.*, CeO<sub>2</sub>/ZnO, NiO/ZnO, CuO/ZnO modified semiconductor nano heterostructures have been carried out with an aim to obtain data for treating model dye effluents. Effect of various operational parameters (like initial concentration of dye, dose of catalyst, initial pH of dye solution and irradiation time have been investigated for fixing the optimum conditions for maximum percentage degradation of GV dye at room temperature. The photodegradation percentage decreased with increasing the initial concentration of dye and increased with increasing the dose of the catalyst, contact time and initial pH for GV dye. As a result of the above parameters, it is concluded that the mineralization of wastewater is varies with varying the initial pH of dye solutions. The photodegradation studies have been carried out under visible light radiations. This work has been carried out with an aim to obtain data for treating industrial effluents from textile industries.

The CeZn<sub>2</sub>O<sub>4</sub> nanocomposites material have been prepared and characterized by FESEM, PXRD and UV-DRS analysis. The UV-DRS shows an increasing absorption in the visible region. The

FESEM results were confirming the formation of  $\text{CeZn}_2\text{O}_4$  nanocomposites are nanospheres and all spheres has good uniform diameter size of about 0.4 micron. XRD thus confirms that the obtained nanomaterial is the combination of  $\text{CeO}_2$  and wurtzite hexagonal well-crystalline  $\text{ZnO}$ .  $\text{CeZn}_2\text{O}_4$ /Visible light system exhibited superior photocatalytic degradation of BG dye than that of  $\text{ZnO}$ /Visible light system. Therefore, because of its promising and enhanced photocatalytic degradation performance, this can be effectively used for future environmental applications.